

## LETTERS

# Triggering of New Madrid seismicity by late-Pleistocene erosion

E. Calais<sup>1</sup>, A. M. Freed<sup>1</sup>, R. Van Arsdale<sup>2</sup> & S. Stein<sup>3</sup>

The spatiotemporal behaviour of earthquakes within continental plate interiors is different from that at plate boundaries. At plate margins, tectonic motions quickly reload earthquake ruptures, making the location of recent earthquakes and the average time between them consistent with the faults' geological, palaeoseismic and seismic histories. In contrast, what determines the activation of a particular mid-continental fault and controls the duration of its seismic activity remains poorly understood<sup>1</sup>. Here we argue that the concentration of magnitude-7 or larger earthquakes in the New Madrid seismic zone of the central United States<sup>2,3</sup> since the end of the last ice age results from the recent, climate-controlled, erosional history of the northern Mississippi embayment. We show that the upward flexure of the lithosphere caused by unloading from river incision between 16,000 and 10,000 years ago caused a reduction of normal stresses in the upper crust sufficient to unclamp pre-existing faults close to failure equilibrium. Models indicate that fault segments that have already ruptured are unlikely to fail again soon, but stress changes from sediment unloading and previous earthquakes may eventually be sufficient to bring to failure other nearby segments that have not yet ruptured.

Large earthquakes within continents, far from plate boundaries, are episodic, clustered and seem to migrate through time. Although this behaviour is recognized in many continental interiors<sup>1</sup>, the best-studied case is the New Madrid seismic zone (NMSZ) in the central United States (Fig. 1), which was struck by three magnitude-7 or greater earthquakes in 1811–1812<sup>2,3</sup>. Smaller earthquakes continue today, outlining the fault segments thought to have ruptured in 1811–1812, and palaeoseismic records show evidence of large events about 500 yr apart in the past 2 kyr (ref. 4). The occurrence of such large earthquakes in the stable continental interior, far from plate boundaries, had been taken as evidence that strain accumulates steadily on the New Madrid faults and is periodically released during large, infrequent events. However, 20 yr of Global Positioning System (GPS) measurements find no detectable deformation, with progressively higher precision, constraining any present motions across the NMSZ to be slower than  $0.2 \text{ mm yr}^{-1}$  (refs 5,6). Because known large earthquakes in the NMSZ are equivalent to an elastic strain release rate of at least  $1\text{--}2 \text{ mm yr}^{-1}$  over the past  $\sim 2$  kyr, this indicates that deformation rates vary with time and precludes a steady-state model where the recurrence of large earthquakes removes the strain accumulating at approximately the same rate.

Hence, the NMSZ must have been recently activated, consistent with the lack of significant topography in the region and with seismic reflection and trenching studies that find an increase in slip rate on the Reelfoot fault by four orders of magnitude about 10 kyr ago<sup>7</sup>. This recent reactivation of the NMSZ argues against Holocene fault activity being a direct manifestation of tectonic stresses, which change on timescales of millions of years. A similar conclusion emerges from

the observation that plate-wide GPS measurements in stable North America, Europe and Australia (outside the areas currently affected by glacial isostatic adjustment) also show very low deformation rates, of less than  $0.5 \text{ mm yr}^{-1}$  over 5,000 km (ref. 8). In the absence of significant far-field displacement loading and regional-scale strain accumulation, what determines the occurrence of large earthquakes in plate interiors remains unknown. The North American plate interior contains many fossil faults that developed at different times with different orientations, but only a few seem active today. Hence, although the earthquakes probably occur by reactivation of favourably oriented faults associated with Palaeozoic rifting, a localized stress source must have recently triggered these particular faults. Similarly, although slowly varying plate-wide or regional forces may have a role in New Madrid seismicity, the primary triggers must be localized in space and time.

Various local stress sources have been explored so far. For instance, it has been proposed that the recent activation of the NMSZ, coincident

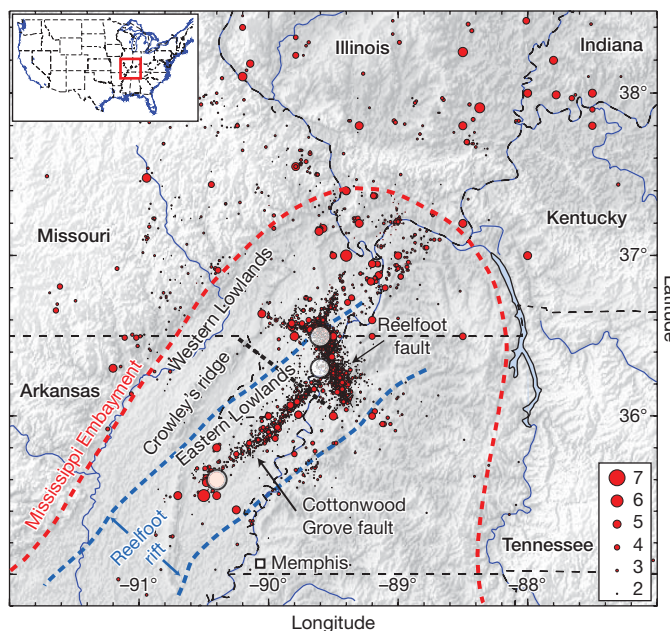


**Figure 1 | Current seismicity of the NMSZ.** Red circles show National Earthquake Information Center (NEIC) and Center for Earthquake Research and Information catalogues (1974 to present), and white circles show the location of the 1811–1812 events from the NEIC catalogue of significant historical events. Circle size corresponds to earthquake magnitude, as indicated. The red dashed line shows the perimeter of the Mississippi embayment, and the Palaeozoic Reelfoot rift is schematically delimited by the two blue dotted lines. The black dashed line shows the location of the cross-section in Fig. 2.

<sup>1</sup>Purdue University, Department of Earth and Atmospheric Sciences, West Lafayette, Indiana 47907, USA. <sup>2</sup>University of Memphis, Department of Earth Sciences, Memphis, Tennessee 38152, USA. <sup>3</sup>Northwestern University, Department of Earth and Planetary Sciences, Evanston, Illinois 60208, USA.

with the end of the last ice age, resulted from stress changes caused by the melting of the Laurentide ice sheet<sup>9</sup>. However, because flexural stresses decay rapidly away from the ice margin, this mechanism fails to explain fault activation in the NMSZ<sup>10</sup> unless its upper mantle and lower crust are an order of magnitude weaker than the surroundings<sup>9</sup>. Such a lateral variation in viscosity is unlikely given the absence of a heat flow anomaly<sup>11</sup>. A similar difficulty arises for models in which seismicity results from sinking of an ancient high-density mafic body<sup>12,13</sup> or from a sudden weakening of the lower crust<sup>14</sup> in the past 9 kyr (ref. 13), because there is no evidence for such a weak zone and no obvious mechanism for the weakening. In summary, no single model has so far been able to explain simultaneously the spatial concentration of large earthquakes in the NMSZ, their temporal clustering in the past ~10 kyr and the absence of measureable contemporary strain accumulation in the region. Here we argue that the onset of fault activity coincidental with the end of the last ice age, and the concentration of large earthquakes in the NMSZ since then, results from stress changes caused by the upward flexure of the lithosphere associated with river incision in the northern Mississippi embayment at the end of the Pleistocene epoch<sup>15</sup>.

The NMSZ (Fig. 1) occupies the eastern part of the upper Mississippi embayment and coincides with part of the Cambrian Reelfoot rift. During most of the Pleistocene, the ancestral Mississippi River flowed south through the Western Lowlands and the ancestral Ohio River flowed south through the Eastern Lowlands, with Crowley's ridge as the drainage divide between the two lowlands. The geologic history of the ancestral Ohio River preserved in the Eastern Lowlands since the end of the Pleistocene (Fig. 2) consists of late-Wisconsin (19.7 kyr BP) formation of the Sikeston flood plain by aggradation or entrenchment through a higher flood plain that was not preserved; minor entrenchment and formation of the late-Wisconsin (16.1 kyr BP) Kennett flood plain; latest-Wisconsin (12.4 kyr BP) entrenchment of the eastern two-thirds of the Eastern Lowlands and formation of the Morehouse flood plain; and entrenchment through the Morehouse flood plain by the Mississippi River to the current flood-plain elevation, which occurred 10.1 kyr BP<sup>16</sup>. This late-Pleistocene evolution of the central Mississippi River valley, which was controlled by deglacial melt water and outwash at the transition from glacial to interglacial conditions, therefore removed about 6 m of sediments over a 60-km-wide area between about 16 and 12 kyr BP, followed by the removal of another 6 m over a 30-km-wide area between about 12 and 10 kyr BP. The most recent incision event is coincident with and was caused by the northwards stepping of the confluence of the Mississippi and Ohio rivers to its current location at Cairo, Illinois<sup>16</sup>. Thus, the late-Pleistocene denudation is temporally and spatially unique to the central and lower Mississippi River valley.

To test whether the removal of this load is sufficient to activate faulting in the NMSZ, we developed a finite-element model that simulates

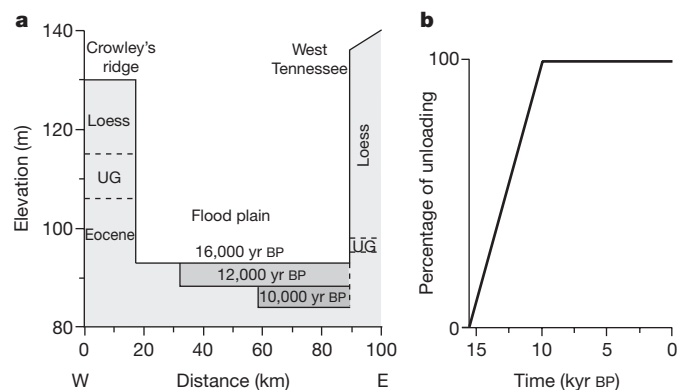


**Figure 2 | Late-Pleistocene sedimentary history.** **a**, Schematic west-east cross-section across the Eastern Lowlands near latitude 36° showing the three successive flood plains. UG, Pliocene Upland Complex gravel. **b**, Unloading history used here. The model accounts for the eastwards migration of the region of unloading through time shown in **a**.

a negative surface pressure associated with sediment removal, allowing a viscoelastic lower crust and mantle to relax both during and after removal of this load (Methods). In the absence of additional details on the erosional history, we use a simple unloading model where sediments are removed at a constant rate in two steps (Fig. 2a).

The sediment removal induces flexural uplift that, in turn, causes stress increase (that is, towards extension) above a neutral axis (at a depth of ~28 km here) and stress decrease (towards compression) below (Fig. 3). Tensional stress changes are largest in the seismogenic upper crust at depths between 5 and 15 km, where current seismicity occurs. These act to reduce the net compressive normal (clamping) force that keeps faults striking perpendicular to the model profile from slipping, therefore bringing these faults closer to failure. Such basin-parallel faults include the Cottonwood Grove fault (Fig. 1), which ruptured first during the 1811–1812 sequence<sup>17</sup>. Stress changes of a few 0.1 MPa, although relatively small, are well within the range assumed to trigger earthquakes on critically loaded faults<sup>18</sup>. Critical loading is expected for a state of stress where intraplate continental crust is in a state of failure equilibrium<sup>19</sup>. These stress changes would also promote failure on other basin-parallel faults within the Mississippi embayment that may have ruptured in the 1811–1812 earthquakes (such as the New Madrid North fault<sup>20</sup>), on the Bootheel lineament<sup>21</sup> or on those along the southeastern margin of the Reelfoot rift that show Quaternary faulting events<sup>22</sup>. These simulations predict very small present-day horizontal strain rates ( $<2 \times 10^{-10} \text{ yr}^{-1}$ ; Supplementary Fig. 3, top) and total vertical displacements ( $<2 \text{ m}$  over 150 km; Supplementary Fig. 3, bottom) that are much smaller than the current detection threshold of geodetic or geological observations and, hence, consistent with the lack of evidence for significant vertical or horizontal strain accumulation across the NMSZ today<sup>6</sup>.

Although sediment unloading is assumed to be linear from 16 to 10 kyr BP and zero thereafter, the stress build-up has a more complicated time history owing to mantle relaxation (Fig. 4). The weaker-rheology model leads to faster stress changes with time and reduces the normal stress by about 0.4 MPa over the 16-kyr period covered by the calculation, with a current rate of about 0.02 MPa per kiloyear. In contrast, the strongest endmember model reduces the normal stress by less than 0.15 MPa over the past 16 kyr, and by an insignificant rate since the time of sediment unloading. The endmember case of instantaneous unloading 16 kyr BP for the weak rheology (Fig. 4b) provides an upper

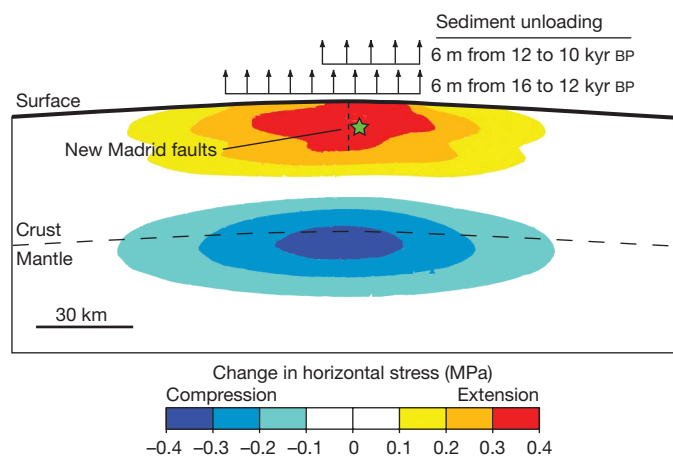


**Figure 3 | Horizontal stress changes due to flexure.** Colours show the model horizontal stress changes due to flexure associated with sediment unloading and associated viscoelastic relaxation using the weakest-rheology endmember model (Fig. 4). Unloading is modelled as a negative pressure at the surface in a two-step process across the region shown in the figure. Deformation is exaggerated by a factor of 5,000. The star marks the location where calculated stress time histories shown in Fig. 4b are sampled. The lower elastic strength of sediments (Supplementary Table 1) prevents extensional stresses from being greatest at the surface. Only a portion of the full model domain (200 km deep, 1,500 km wide) is shown.

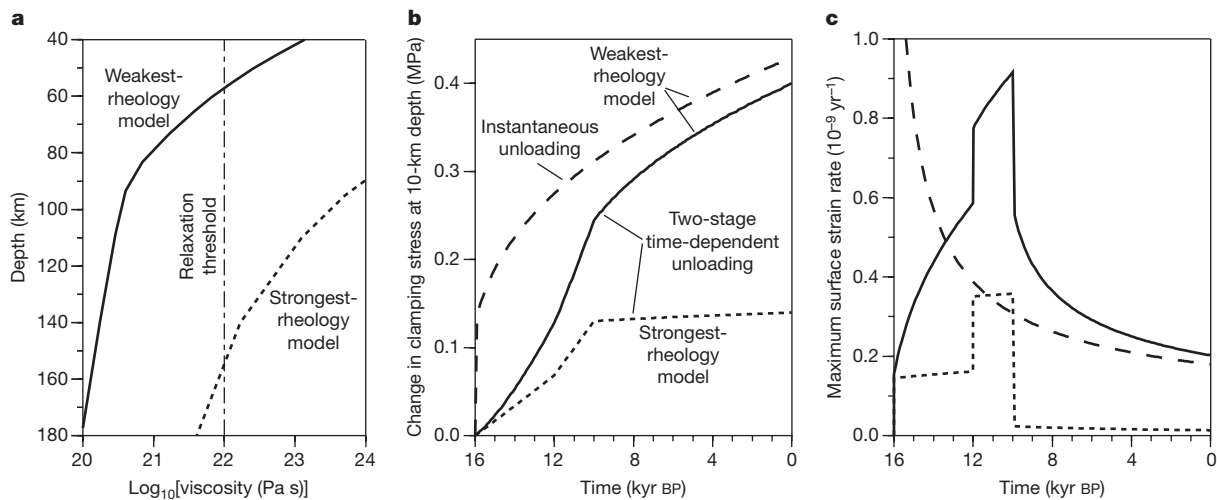


**Figure 4 | Effect of rheology and unloading history.** **a**, Endmember rheologies corresponding to equivalent flexural thicknesses (depth where a viscosity of  $10^{22}$  Pa s is reached) of  $\sim 60$  and  $\sim 150$  km, respectively, displaying the wide range of potential strength profiles. The weakest-rheology model is based on an Anita Bay dunite mantle with activation energy  $Q = 420 \text{ kJ mol}^{-1}$  (lowest of experimental range) and a thermal gradient associated with a heat flow of  $62 \text{ mW m}^{-2}$  (highest of observational range). The strongest-rheology model is based on a dry dunite mantle with  $Q = 568 \text{ kJ mol}^{-1}$  (highest of experimental range) and a thermal gradient

bound for uncertainties in the unloading history. Larger stress reductions occur earlier, but by now are close to the time-dependent unloading case. Both cases, however, lead to similar contemporary stressing rates.

The comparison between the clamping stress history for the weakest and strongest rheologies (Fig. 4b) illustrates how viscous relaxation amplifies the flexural stress changes. In the strongest-rheology case (155-km equivalent elastic thickness), very little viscous relaxation occurs. Hence, the unclamping stress increases linearly as the load is removed, after which it remains constant, not exceeding  $\sim 0.15$  MPa. In the case of weaker rheologies, the effective elastic thickness of the lithosphere decreases with time as flexural stresses relax. Because flexural rigidity is proportional to the cube of the elastic thickness, this thinning translates into a significant increase in flexural displacements and stresses, the latter reaching up to 0.4 MPa today. This process leads to the continued build-up of stresses long after unloading of sediments is complete because the unloading occurs over a period similar to the relaxation time of the sublithospheric mantle (viscosity divided by shear modulus). Below a depth of  $\sim 60$  km, mantle relaxation times for the weak-endmember model are 7 kyr or less, comparable to the duration of the late-Wisconsin erosional event.

The simple flexural mechanism proposed here explains the activation of the NMSZ faults  $\sim 10$  kyr ago. It does not require an *ad hoc* thermal weakening of the lower crust or upper mantle, for which there is no direct evidence. It predicts small current strain rates consistent with geodetic observations. The triggering mechanism is the previously recognized erosion of alluvial sediments during rapid climate change at the transition from the last ice age into the Holocene epoch. To be effective, this process requires the dissipation of flexural stresses in a viscoelastic upper mantle with a relaxation time of the order of several thousand years. Hence, in this model climate variations and mantle rheology jointly control the activation of crustal faulting in the NMSZ. The model requires an erosional perturbation and a large fault at failure equilibrium (Reelfoot rift), both of which are documented. These requirements, met in the upper Mississippi embayment, need not imply that the NMSZ is the only reactivated mid-continent rift zone, merely that it is the only one in which large Holocene earthquakes have been documented.

associated with a heat flow of  $46 \text{ mW m}^{-2}$  (lowest of observational range). **b**, Reduction in clamping stress at a depth of 12 km beneath the load centre (star in Fig. 3), plotted as a function of time for two endmember models that respectively represent the mantle rheologies that are probably weakest (solid line, weakest mineralogy and hottest geotherm) and strongest (dotted line, strongest mineralogy and coolest geotherm), as well as for the case of instantaneous unloading 16 kyr ago (dashed line). **c**, Maximum horizontal strain rate at the surface of the model at the fault location shown in Fig. 3, plotted as a function of time for the same three cases shown in **b**.

The model predicts that faults in the NMSZ continue being unclamped by the relaxation process even 10 kyr after alluvial denudation stopped, although at a slow, decaying rate much less than the rate at which plate boundary faults are loaded by steady plate motion ( $\sim 10$  MPa per kiloyear for the San Andreas fault, for instance<sup>23</sup>). In addition, the maximum amount of stress that can be transferred into the upper crust from viscoelastic relaxation following a shallow magnitude-8 event, given the rheology used here, is of the order of 0.1 MPa per kiloyear<sup>24</sup>, which is more than one order of magnitude less than typical stress-drop values (1–10 MPa) for continental-interior earthquakes<sup>25</sup>. As a consequence, once a large earthquake has released stresses on an intraplate fault segment, flexure and viscoelastic relaxation are inefficient at bringing the rupture back to failure equilibrium.

Hence, fault segments within the NMSZ that have already ruptured are unlikely to fail again soon, although stress changes from erosional unloading or large earthquakes may eventually bring to failure other nearby segments that have not yet ruptured<sup>26</sup>. These stress changes would therefore be incapable of producing, on a single fault segment, the multiple Holocene events documented by palaeoseismic data<sup>4</sup> in the upper Mississippi embayment unless the fault weakens with time, allowing failure at lower stress levels<sup>26</sup>. Otherwise, because strain from far-field motions is currently not accumulating fast enough to account for these events<sup>6</sup>, Holocene seismic activity in the upper Mississippi embayment must be releasing elastic strain energy that accumulated at some time in the past, perhaps associated with the development of high topography both to the east (Mid-Atlantic Ridge) and west (Western Cordillera). In this picture, existing faults from the old Reelfoot rift system are reactivated by small stress changes from erosion-induced flexure. After an initial earthquake, further flexure and coseismic stress changes combine to generate a sequence on closely spaced fault segments within the Reelfoot rift, drawing elastic energy from the long-lived strain reservoir. This process may be what caused seismicity to migrate about the Reelfoot Rift in the past and may eventually activate yet-unruptured segments.

## METHODS SUMMARY

We calculated stress changes due to the removal of sediments using the finite-element program ABAQUS with a two-dimensional plane-strain geometry, fixed boundary conditions along the bottom and sides, and a temperature-dependent viscoelastic rheology with dislocation creep. The thermal gradient was calculated

from observed heat flow using thermal conductivity and heat production rates adopted by previous authors. The background stress rate was derived from the maximum horizontal strain rate in the New Madrid region, as constrained by the most current GPS measurements.

**Full Methods** and any associated references are available in the online version of the paper at [www.nature.com/nature](http://www.nature.com/nature).

**Received 12 October 2009; accepted 7 June 2010.**

1. Crone, A. J., De Martini, P. M., Machette, M. N., Okumura, K. & Prescott, J. R. Paleoseismicity of two historically quiescent faults in Australia: implications for fault behavior in stable continental regions. *Bull. Seismol. Soc. Am.* **93**, 1913–1934 (2003).
2. Johnston, A. C. Seismic moment assessment of earthquakes in stable continental regions. III. New Madrid 1811–1812, Charleston 1886, and Lisbon 1755. *Geophys. J. Int.* **126**, 314–344 (1996).
3. Hough, S. E., Armbuster, J. G., Seeber, L. & Hough, J. F. On the modified Mercalli intensities and magnitudes of the 1811–1812 New Madrid earthquakes. *J. Geophys. Res.* **105**, 23839–23864 (2000).
4. Tuttle, M. *et al.* The earthquake potential of the New Madrid seismic zone. *Bull. Seismol. Soc. Am.* **92**, 2080–2089 (2002).
5. Newman, A. *et al.* Slow deformation and lower seismic hazard at the New Madrid seismic zone. *Science* **284**, 619–621 (1999).
6. Calais, E. & Stein, S. Time-variable deformation in the New Madrid seismic zone. *Science* **323**, 1442 (2009).
7. Van Arsdale, R. B. Displacement history and slip rate on the Reelfoot fault of the New Madrid seismic zone. *Eng. Geol.* **55**, 219–226 (2000).
8. Calais, E., Han, J. Y., DeMets, C. & Nocquet, J. M. Deformation of the North American plate interior from a decade of continuous GPS measurements. *J. Geophys. Res.* **111**, B06402 (2006).
9. Grollimund, B. & Zoback, M. D. Did deglaciation trigger intraplate seismicity in the New Madrid seismic zone? *Geology* **29**, 175–178 (2001).
10. Wu, P. & Johnston, P. Can deglaciation trigger earthquakes in North America? *Geophys. Res. Lett.* **27**, 1323–1326 (2000).
11. McKenna, J., Stein, S. & Stein, C. A. Is the New Madrid seismic zone hotter and weaker than its surroundings? *Spec. Pap. Geol. Soc. Am.* **425**, 167–175 (2007).
12. Grana, J. P. & Richardson, R. M. Tectonic stress within the New Madrid seismic zone. *J. Geophys. Res.* **101**, 5445–5458 (1996).
13. Pollitz, F. F., Kellogg, L. & Burgmann, R. Sinking mafic body in a reactivated lower crust: a mechanism for stress concentration at the New Madrid seismic zone. *Bull. Seismol. Soc. Am.* **91**, 1882–1897 (2001).
14. Kenner, S. J. & Segall, P. A mechanical model for intraplate earthquakes: application to the New Madrid seismic zone. *Science* **289**, 2329–2332 (2000).
15. Van Arsdale, R., Bresnahan, R., McCallister, N. & Waldron, B. Upland Complex of the central Mississippi River valley: its origin, denudation, and possible role in reactivation of the New Madrid seismic zone. *Geol. Soc. Am. Spec. Pap.* **425**, 77–192 (2007).
16. Rittenour, T. M., Blum, M. D. & Goble, R. J. Fluvial evolution of the lower Mississippi River valley during the last 100 k.y. glacial cycle: response to glaciations and sea-level change. *Geol. Soc. Am. Bull.* **119**, 586–608 (2007).
17. Mueller, K., Hough, S. E. & Bilham, R. Analysing the 1811–1812 New Madrid earthquakes with recent instrumentally recorded aftershocks. *Nature* **429**, 284–287 (2004).
18. Freed, A. M. Earthquake triggering by static, dynamic, and postseismic stress transfer. *Annu. Rev. Earth Planet. Sci.* **33**, 335–367 (2005).
19. Townend, J. & Zoback, M. D. How faulting keeps the crust strong. *Geology* **28**, 399–402 (2000).
20. Baldwin, J. N. *et al.* Constraints on the location of the late Quaternary Reelfoot and New Madrid North faults in the northern New Madrid seismic zone, central United States. *Seismol. Res. Lett.* **6**, 772–789 (2005).
21. Guccione, M. J., Marple, R. & Autin, W. J. Evidence for Holocene displacements on the Bootheel fault (lineament) in southeastern Missouri: seismotectonic implications for the New Madrid region. *Geol. Soc. Am. Bull.* **117**, 319–0333 (2005).
22. Cox, R. T., Harris, J., Larsen, J. B., Van Arsdale, R. B. & Forman, S. L. Paleoseismology of the southeastern Reelfoot Rift in western Tennessee and implications for intraplate fault zone evolution. *Tectonics* **25**, TC3019 (2006).
23. Freed, A. M., Ali, S. T. & Bürgmann, R. Evolution of stress in Southern California for the past 200 years from coseismic, postseismic and interseismic stress changes. *Geophys. J. Int.* **169**, 1164–1179 (2007).
24. Freed, A. M., Bürgmann, R., Calais, E., Freymueller, J. & Hreinsdóttir, S. Implications of deformation following the 2002 Denali, Alaska, earthquake for postseismic relaxation processes and lithospheric rheology. *J. Geophys. Res.* **111**, B01401 (2006).
25. Allmann, B. P. & Shearer, P. M. Global variations of stress drop for moderate to large earthquakes. *J. Geophys. Res.* **114**, B01310 (2009).
26. Li, Q., Liu, M. & Stein, S. Spatial-temporal complexity of continental intraplate seismicity: insights from geodynamic modeling and implications for seismic hazard estimation. *Bull. Seismol. Soc. Am.* **99**, 52–60 (2009).

**Supplementary Information** is linked to the online version of the paper at [www.nature.com/nature](http://www.nature.com/nature).

**Acknowledgements** This work was partly supported by the US Geological Survey through the Department of the Interior, under USGS award number 07HQGR0049. We thank M. Zoback for his comments.

**Author Contributions** E.C. designed the study and prepared the main manuscript, with contributions from all co-authors. A.M.F. performed the modelling tasks and wrote Methods. R.V.A. provided the geological information. S.S. provided background context for the study. All authors discussed the results and implications and commented on the manuscript at all stages.

**Author Information** Reprints and permissions information is available at [www.nature.com/reprints](http://www.nature.com/reprints). The authors declare no competing financial interests. Readers are welcome to comment on the online version of this article at [www.nature.com/nature](http://www.nature.com/nature). Correspondence and requests for materials should be addressed to E.C. ([ecalais@purdue.edu](mailto:ecalais@purdue.edu)).

## METHODS

We use the finite-element program ABAQUS (<http://www.simulia.com>), a code widely used for nonlinear engineering applications, to build and solve a two-dimensional plane-strain model. This geometry is justified by the significant length and fairly linear course of the Mississippi River valley through the New Madrid region. The model is 200 km deep and 1,500 km wide, with fixed boundary conditions along the bottom and sides. Testing shows that these boundaries are at sufficient distance not to influence model results. We simulate the removal of a 12-m-thick,  $2,000 \text{ kg m}^{-3}$  layer of sediment in a two-step process with an equivalent negative pressure applied over the appropriate region of the river valley. We also tested an endmember unloading model where the entire load is instantly removed at 16 kyr BP. Elastic parameters are as listed in Supplementary Table 1.

Viscoelastic properties in the lower crust and uppermost mantle are governed by dislocation creep<sup>27</sup>, which laboratory rock-squeezing experiments show to be characterized by a power-law relation where strain rate is proportional to stress raised to a certain power<sup>28,29</sup>:

$$\dot{\epsilon} = A\sigma^n e^{-Q/RT}$$

Here  $\dot{\epsilon}$  is strain rate ( $\text{s}^{-1}$ ),  $A$  is a pre-exponential factor ( $\text{MPa}^{-n} \text{ s}^{-1}$ ),  $\sigma$  is the differential stress (MPa),  $n$  is the stress exponent,  $Q$  is the activation energy ( $\text{kJ mol}^{-1}$ ),  $T$  is temperature (K) and  $R$  is the universal gas constant ( $\text{J mol}^{-1} \text{ K}^{-1}$ ). In terms of viscosity (Pa s)

$$\eta = \sigma^{1-n} e^{Q/RT} / 2A$$

Dislocation creep is ultimately controlled by the lithospheric thermal gradient, mineralogy and differential stress. We calculated the thermal gradient from the observed heat flow in the Reelfoot rift ( $55 \pm 7 \text{ mW m}^{-2}$ ) using the thermal conductivity and heat production rates adopted by previous authors<sup>30</sup> (Supplementary Table 1). Uncertainty in heat flow leads to calculated thermal gradients that imply temperatures ranging from 630 °C to 930 °C at 60-km depth (Supplementary Fig. 1). We used power-law parameters for various crustal and

mantle mineralogies (Supplementary Table 2 and Supplementary Fig. 2) as proposed by previous authors<sup>30</sup>.

The most significant parameter range is that of activation energy, which controls the sensitivity of viscosity to temperature. The lower the activation energy, the lower the effective viscosity for a given thermal gradient. Supplementary Fig. 2 shows the sensitivity of viscosity as a function of assumed mineralogy for a nominal ( $55 \text{ mW m}^{-2}$ ) thermal gradient and a background strain rate of  $10^{-9} \text{ yr}^{-1}$ , with ranges shown for laboratory uncertainties in activation energy.

Model results indicate that rheologies with viscosities greater than  $\sim 10^{22} \text{ Pa s}$  (labelled 'relaxation line' in Supplementary Figure 2) do not significantly relax flexural stresses associated with sediment unloading in the time frame of this analysis (16 kyr BP). This includes the entire crust, meaning that its viscoelastic strength is too high for it to have a significant role in the response of the lithosphere to sediment unloading.

Differential stress is comprised of background plus flexural stress components. Here, background stress levels are generally larger than the small stress changes associated with sediment removal. Thus, the viscosity structure is primarily controlled by the background stress, which we derive from the background strain rate across the region. With power-law exponents typically of between three and four, higher strain rates (higher background stress) lead to lower effective viscosities. The maximum horizontal strain rate in the New Madrid region, as constrained by the most current GPS measurements<sup>6</sup>, is  $\sim 10^{-9} \text{ yr}^{-1}$ . We assume this value in all of our calculations. Lower background strain rates would translate into higher effective viscosities and a stronger lithosphere. The stress changes calculated here therefore represent an upper bound with respect to background strain rate.

27. Karato, S. I. in *Earth's Deep Interior* (ed. Croosley, D.) 223–272 (Gordon and Breach, 1997).
28. Carter, N. L. & Tsenn, M. C. Flow properties of continental lithosphere. *Tectonophysics* **136**, 27–63 (1987).
29. Kirby, S. H. & Kronenberg, A. K. Rheology of the lithosphere; selected topics. *Rev. Geophys.* **25**, 1219–1244 (1987).
30. Liu, L. & Zoback, M. D. Lithospheric strength and intraplate seismicity in the New Madrid seismic zone. *Tectonics* **16**, 585–595 (1997).